

Nitric Oxide Switches on the Photoluminescence of Molecularly Engineered Quantum Dots

Suhua Wang,[†] Ming-Yong Han,[‡] and Dejian Huang^{*†}

Department of Chemistry, National University of Singapore, Singapore 117543, Division of Bioengineering, National University of Singapore, Singapore 117576, and Institute of Materials Research and Engineering, A *STAR, Singapore 117602

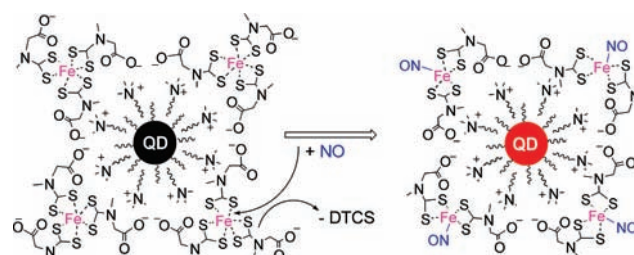
Received June 12, 2009; E-mail: chmhdj@nus.edu.sg

The discovery that mammalian cells have the ability to synthesize the free radical nitric oxide (NO) has triggered an extraordinary impetus for scientific research in all the fields of biology and medicine.¹ Sensitive and selective detection of short-lived NO is a great challenge, and research progress on NO in biology and medicine field has heavily relied on the development of suitable detection methods and molecular probes.² Quantum dots (QDs) have superior luminescence properties and can be molecularly engineered as chemosensors through grafting, on the surface of QDs, a layer of organic molecules that are responsive toward analytes by switching the luminescence on/off.³ Here we show an unprecedented example of an energy-transfer-based photoluminescence (PL) nanoprobe for selective and quantitative detection of nitric oxide, through molecular engineering of the superior optical properties of inorganic QDs by iron complexes which have a unique reactivity to NO.

To detect NO selectively and sensitively, the functional moiety of the probe should react with NO directly, rapidly, and stoichiometrically; the spectroscopic property should also change dramatically for easy monitoring. Tris(dithiocarbamato)iron(III) complex has been shown to possess such a feature, as it rapidly reacts with NO through electron transfer and a ligand substitution reaction to give paramagnetic bis(dithiocarbamato)nitrosyliron(I). This reaction has been broadly utilized for *in vivo* ESR detection of NO.⁴ The NO concentrations are linearly correlated to the ESR signal intensities of the paramagnetic Fe(NO) complexes because of the quantitative and fast (second-order reaction rate is on the order of $10^8 \text{ M}^{-1} \cdot \text{s}^{-1}$) NO trapping efficiency by the ferric complex.⁵ The ESR approach is however not commonly accessible and suitable for real time monitoring and also requires tedious sample preparation steps. For practicality, the use of a “switch-on” fluorescent probe with a short response time is preferred, as it allows real time monitoring in living systems. We noticed that the deep red color of tris(dithiocarbamato)iron(III) faded away rapidly when it was exposed to nitric oxide as was observed previously.⁶ We took advantage of this optical phenomenon to assemble a functional QD consisting of CdSe–ZnS nanocrystals and tris(dithiocarbamato)iron(III) for sensing nitric oxide through a fluorescence “switching on” mechanism. A prototype of such materials was fabricated by grafting tris(*N*-(dithiocarboxy)sarcosine)iron(III) ($[\text{Fe}(\text{DTCS})_3]^{3-}$) on the surface of QDs through an ionic bond as shown in Scheme 1. The hydrophobic trioctylphosphine oxide capped CdSe–ZnS QD cores were stabilized within the cetyltrimethylammonium cationic micelles prepared through ion exchange between $(\text{NH}_4)_3\text{Fe}(\text{III})\text{-(DTCS)}_3$ and cetyltrimethylammonium hydroxide or, more conveniently, cetyltrimethylammonium bromide due to its relative high

degree of counterion binding ($\beta = \sim 0.7$) of carboxylate in the dithiocarbamate.⁷

Scheme 1. Nonfluorescent CdSe–ZnS QDs Are Turned on by Nitric Oxide to Emit Red Photoluminescence^a



^a The scheme illustrates the structure of the nanoprobe consisting of QDs as the fluorophore and surface bound iron(III) dithiocarbamates as the reactive centers.

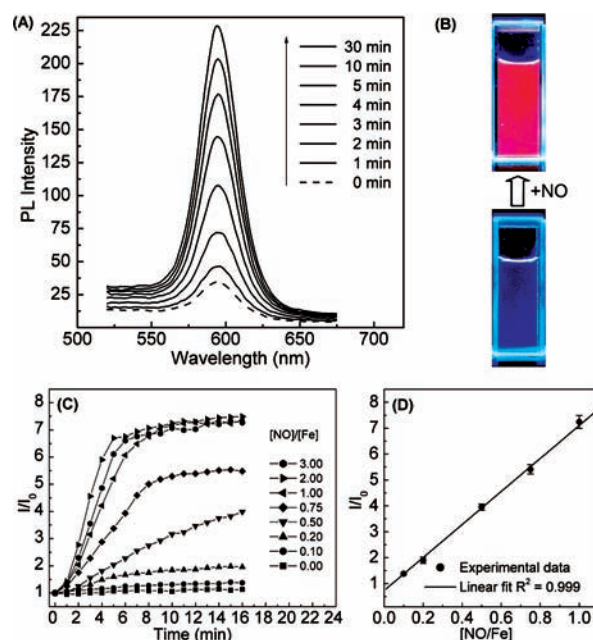


Figure 1. (A) Change of PL spectra of the nanoprobe with time upon addition of nitric oxide. (B) Images of the nanoprobe solution under 320 nm irradiation before and after nitric oxide addition. (C) Increments of PL intensity of the nanoprobe against time after the addition of different amount of nitric oxide. (D) Dosage increments of the nanoprobe’s PL intensity obtained 15 min after nitric oxide addition.

We nickname the nanocomposite “Fe(III)-QD-nanoprobe” from here on for easy communication. The Fe(III)-QD-nanoprobe is easy to assemble and reproducible in terms of performance on nitric

[†] Department of Chemistry, National University of Singapore.

[‡] Division of Bioengineering, National University of Singapore, and A *STAR.

oxide sensing because the ionic interaction eliminates the need for surface trioctylphosphine oxide replacement and protects the fluorescence property of the QDs.

The Fe(III)-QD-nanoprobe initially showed very weak fluorescence (Figure 1A, dashed curve) because of the quenching effect of the surface bound $[\text{Fe}(\text{DTCS})_3]^{3-}$, which had electronic spectra that overlap with the QDs' emission and excitation wavelengths (Figure 2). The anionic $[\text{Fe}(\text{DTCS})_3]^{3-}$ was much more effective to quench the QDs' fluorescence than its neutral analogue with dimethyldithiocarbamate as ligand in solution (Figure S1), confirming the crucial role of surface bonding in switching off the fluorescence. Addition of only NO to CTAB coated water-soluble QDs without $[\text{Fe}(\text{DTCS})_3]^{3-}$ led to minimal fluorescence decrease (Figure S2). Upon addition of 2-(*N,N*-diethylamino)-diazolate-2-oxide diethylammonium salt (DEA/NO, NO donor), the fluorescence intensity of the Fe(III)-QD-nanoprobe solution was switched on and reached its maximum within 30 min (Figure 1A, solid curves). The red fluorescence was easily visualized from the images of the solution after addition of DEA/NO to the Fe(III)-QD-nanoprobe solution (Figure 1B). As a further confirmation to this result, addition of aqueous nitric oxide solution to the nanoprobe solution also switched on the fluorescence immediately. DEA/NO was selected as a NO source for the remaining experiments because its concentration could be easily controlled and was more accurate as compared to aqueous NO solution, which was highly sensitive to air and led to concentration change over time.

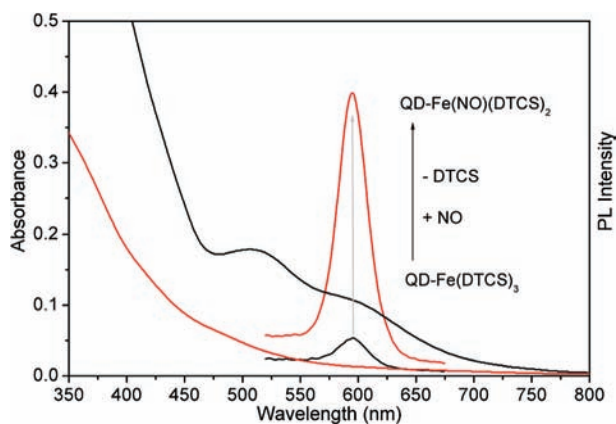


Figure 2. UV-vis absorption spectra of the Fe(III)(DTCS)₃ (black) before and (red) after the addition of nitric oxide. The photoluminescence spectra of the nanoprobe (black) before and (red) after the addition of nitric oxide. The PL intensities were normalized with respect to the absorbance.

The dose dependent kinetic curves of the reaction shown in Figure 1C reveal a 1:1 stoichiometry between NO and Fe. The fluorescence enhancement behavior with time is in agreement with the NO release kinetics of DEA/NO which has a half-life of several minutes at room temperature.⁸ The fluorescence was enhanced by more than 7 times after 10 min of 1 equiv of DEA/NO. More precisely, the fluorescence quantum yields of the probes increased more than 10 times ($QY = 8.7\%$) as measured at 30 min after exposure to NO (Figure S3). The fluorescence was stable up to 1 h but slowly decreased to 75% of the original intensity after 3 h (Figure S4). Addition of more NO only recovered a small fraction of the fluorescence indicating an irreversible change of the probe. For quantitative purposes, the amount of fluorescence increased was also linearly responsive to the concentration of DEA/NO added (Figure 1D). Quantitative analysis of this approach showed a good limit of detection (LOD) for NO at $\sim 3.0 \mu\text{M}$, and the limit of quantification was $\sim 9.0 \mu\text{M}$. This value could be further optimized

by judicious selection of a proper combination of the metal complexes and the QDs as well as by shortening of the distance between the QDs and the metal complexes.

We proposed that the working principle of Fe(III)-QD-nanoprobe could be explained by the electronic spectra of the metal complexes and the emission spectra of the QDs. The UV-vis spectrum of $[\text{Fe}(\text{DTCS})_3]^{3-}$ shows a broad intramolecular charge transfer absorption peak around 595 nm ($\epsilon = 1350 \text{ M}^{-1} \text{ cm}^{-1}$),⁹ as shown in Figure 2. This band overlapped with the maximum emission of the QDs facilitating energy transfer from the excited QDs to the surface bound $[\text{Fe}(\text{DTCS})_3]^{3-}$ complexes resulting in the weak fluorescence of Fe(III)-QD-nanoprobe. After the addition of NO, the absorption at 595 nm disappeared and thus shut down the energy transfer pathway and switched on the fluorescence of the QDs (Figure 2). The estimated metal complex and the QD ratio in Fe(III)-QD-nanoprobe was rather high (~ 3000), and the fluorescence quenching was likely achieved by the collective work of many Fe(III) complexes surrounding one QD.

Fe(III)-QD-nanoprobe not only exhibited good sensitivity for the detection of nitric oxide but also showed good selectivity (Figure 3, also Figure S5 for NO, CO, and CN^-). Other π acidic ligands (CO and CN^-), and common biologically important reactive oxygen species (ROS), such as peroxynitrite, hydroxyl radical, hydrogen peroxide, and superoxide, failed to switch on the nanoprobe's fluorescence. Neither nitrite nor nitrate anions switch on the fluorescence of Fe(III)-QD-nanoprobe indicating that the trianionic $[\text{Fe}(\text{DTCS})_3]^{3-}$ was not easily replaced from the surface of the QDs by these monoanions and that NO_2^- and NO_3^- were not reactive toward $[\text{Fe}(\text{DTCS})_3]^{3-}$ under these conditions. Unlike NO, CO and CN^- are not a one-electron reductant. CO did not react with $[\text{Fe}(\text{DTCS})_3]^{3-}$ under the experimental conditions, and CN^- only slightly enhanced the fluorescence intensity.

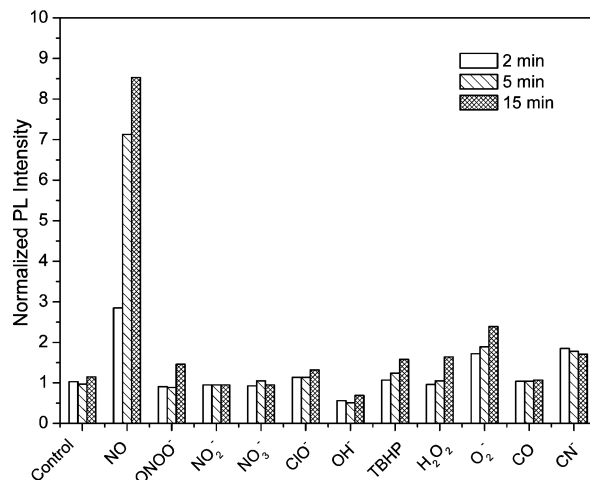


Figure 3. Selectivity of the QDs nanoprobe for NO, determined as the fluorescence response after addition of 3 equiv of these species for 2, 5, and 15 min. $\lambda_{\text{ex}} = 400 \text{ nm}$. All data are normalized with respect to the emission of nanoprobe before the reactive species addition.

The spectroscopic changes of $[\text{Fe}(\text{DTCS})_3]^{3-}$ upon the addition of different ROS such as nitric oxide, hydrogen peroxide, and hypochlorite were investigated to understand the basis of the selectivity. The reaction with hydrogen peroxide caused a small change of absorbance at 595 nm, and ClO^- only slightly decreased the absorbance whereas nitric oxide dramatically decreased the absorbance almost to baseline (Figures S6–S8). These residual absorptions at 595 nm after addition of H_2O_2 and ClO^- suggested that the energy transfer pathways remained possible from the excited QDs and thus could not switch on the QDs' fluorescence effectively.

The ESI-MS spectra (Figure 4 bottom) of the reaction solutions revealed some similarity but marked the difference of the reactions among the ROS with $[\text{Fe}(\text{DTCS})_3]^{3-}$. Nitric oxide reacted with $[\text{Fe}(\text{DTCS})_3]^{3-}$ cleanly to give $[\text{Fe}(\text{I})(\text{NO})(\text{DTCS})_2]^{2-}$ (considering NO as NO^+ ,¹⁰ the angle of Fe–N–O is 172° ¹¹) and an oxidatively dimerized ligand (thiuram disulfide).^{6,12} In contrast, the reaction with hydrogen peroxide swiftly generated thiuram disulfide, *N*-(dithioperoxocarboxy)sarcosine, and uncharacterized iron species. Similar to H_2O_2 , the reaction with hypochlorite also produced thiuram disulfide, *N*-(dithioperoxocarboxy)sarcosine, and an iron(III) complex $[\text{Fe}(\text{III})(\text{DTCS})_2]^{2-}$ at $m/z = 381.9$. The results suggested that H_2O_2 and ClO^- acted merely as oxidants to decompose $[\text{Fe}(\text{III})(\text{DTCS})_3]^{3-}$ with a slight alternation of the absorbance at 595 nm. In sharp contrast, NO acted not only as a one-electron reductant but also as a strong field ligand (in its oxidized form, NO^+) that caused a dramatic blue shift of the UV–vis spectrum. Therefore it could switch on the fluorescence of the QD by shutting down the energy transfer pathway. The oxidation of the lost ligand did not require the presence of oxygen because, under air-free conditions, the reaction still occurred readily. The oxidation of the DTCS to its dimer was likely caused by iron(III), which decreased the oxidation state by two as it apparently received one electron each from NO and DTCS, respectively. The resulting DTCS radical then dimerized to form thiuram disulfide.^{6,12}

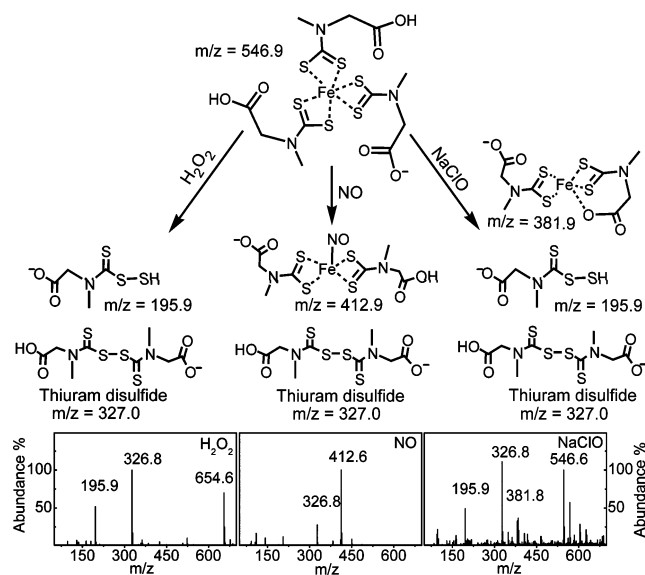


Figure 4. Reaction scheme of $\text{Fe}(\text{III})(\text{DTCS})_3$ with nitric oxide, hydrogen peroxide, and sodium hypochlorite and the corresponding ESI-MS spectra of the resulting solution 5 min after the addition of ROS.

A fluorometric method for NO detection is preferred because it is convenient and has potential for in situ spatial and temporal monitoring of NO generation and bioactivity. Nagano and co-workers developed a series NO probes containing *o*-phenylenediamine derived fluorophores.¹³ The fluorescence of the probe was switched on upon oxidation by dinitrogen trioxide (N_2O_3) which was formed from the NO oxidation in the presence of oxygen. Lippard and co-workers developed an interesting fluorescein-based $\text{Cu}(\text{II})$ complex probe.¹⁴ The fluorescence of the probe was switched on upon reaction with NO by converting the aliphatic amine into nitrosoamine accompanied by the dissociation of the reduced cuprous ion from the complex. The probe was applied in imaging

nitric oxide in living cells.¹⁵ Uncoated CdSe QDs were known to be highly sensitive in the quantification of hydrogen peroxides through the fluorescence quenching mechanism.¹⁶ Yet, there was no report on sensing ROS by the fluorescence “switch-on” mechanism, which is preferred as it has low background interference and higher sensitivity. Our $\text{Fe}(\text{III})$ -QD-nanoprobe described herein can be easily assembled and can be further fine-tuned to achieve even greater sensitivity and compatibility with different settings such as cell line or gaseous nitric oxide measurement in a highly selective and sensitive manner.

In conclusion, we demonstrated here the first example of a fluorescent probe consisting of a transition metal complex and QD in sensing nitric oxide with good sensitivity and excellent selectivity by taking advantage of the strong ligand field property and reducing property of nitric oxide. It is apparent that the combination of the rich optical property of a vast number of transition metal complexes and the desirable fluorescent property of semiconductor QDs may lead to novel probes for sensing reactive oxygen species and small molecule ligands.

Acknowledgment. The authors are grateful for the financial support of the Science and Engineering Research Council (SERC) of the Agency for Science, Technology and Research (A*Star) of Singapore. Grant Number: 072-101-0015. D.H. thanks Ken Caulton for critical comments and suggestions on the manuscript.

Supporting Information Available: Synthesis methods for the nanoprobe and characterization procedures; different ROS sensing procedure with the nanoprobe; UV–vis spectra and absorbance changes at 595 nm upon reaction with different ROS additions; photoluminescence quenching behaviors of QDs by surface bound and free iron dithiocarbamates. This material is available free of charge via the Internet at <http://pubs.acs.org>.

References

- (1) (a) Culotta, E.; Koshland, D. E., Jr. *Science* **1992**, *258*, 1862–1864. (b) Isenberg, J. S.; Martin-Manso, G.; Maxhimer, J. B.; Roberts, D. D. *Nat. Rev. Cancer* **2009**, *9*, 182–194.
- (2) (a) Nagano, T.; Yoshimura, T. *Chem. Rev.* **2002**, *102*, 235–269. (b) Lim, M. H.; Lippard, S. J. *Acc. Chem. Res.* **2007**, *40*, 41–51. (c) Miles, A. M.; Wink, D. A.; Cook, J. C.; Grisham, M. B. *Method Enzymol.* **1996**, *268*, 105–120.
- (3) Zhang, C. Y.; Yeh, H. C.; Kuroki, M. T.; Wang, T. H. *Nat. Mater.* **2005**, *4*, 826–831.
- (4) Yoshimura, T.; Yokoyama, H.; Fujii, S.; Takayama, F.; Oikawa, K.; Kamada, H. *Nat. Biotechnol.* **1996**, *14*, 992–994.
- (5) Fujii, S.; Yoshimura, T.; Kamada, H. *Chem. Lett.* **1996**, 785–786.
- (6) Fujii, S.; Kobayashi, K.; Tagawa, S.; Yoshimura, T. *J. Chem. Soc., Dalton Trans.* **2000**, 3310–3315.
- (7) (a) Jansson, M.; Stils, P. *J. Phys. Chem.* **1987**, *91*, 113–116. (b) Anacker, E. W.; Underwood, A. J. *J. Phys. Chem.* **1981**, *85*, 2463–2466. (c) Toullec, J.; Couderc, S. *Langmuir* **1997**, *13*, 1918–1924.
- (8) Keefer, L. K.; Nims, R. W.; Davies, K. M.; Wink, D. A. *Methods Enzymol.* **1996**, *268*, 281–293.
- (9) (a) Furlani, C.; Luciani, M. L. *Inorg. Chem.* **1968**, *7*, 1586–1592. (b) Coucouvanis, D. In *Progress in Inorganic Chemistry*; Lippard, S. J., Ed.; John Wiley & Sons: New York, 1979; Vol. 26, pp 301–470.
- (10) Ogasawara, M.; Huang, D.; Streib, W. E.; Huffman, J. C.; Gallego-Planas, N.; Maseras, F.; Eisenstein, O.; Caulton, K. G. *J. Am. Chem. Soc.* **1997**, *119*, 8642–8651.
- (11) Davies, G. R.; Jarvis, J. A. J.; Kilbourn, B. T.; Mais, R. H. B.; Owston, P. G. *J. Chem. Soc. A* **1970**, *8*, 1275–1283.
- (12) Fujii, S.; Yoshimura, T. *Coord. Chem. Rev.* **2000**, *198*, 89–99.
- (13) Sasaki, E.; Kojima, H.; Nishimatsu, H.; Urano, Y.; Kikuchi, K.; Hirata, Y.; Nagano, T. *J. Am. Chem. Soc.* **2005**, *127*, 3684–3685.
- (14) Lim, M. H.; Wong, B. A.; Pitcock, W. H.; Mokshagundam, D.; Baik, M.; Lippard, S. J. *J. Am. Chem. Soc.* **2006**, *128*, 14364–14373.
- (15) Lim, M. H.; Xu, D.; Lippard, S. J. *Nat. Chem. Biol.* **2006**, *2*, 375–380.
- (16) Hay, K. X.; Waisundara, V. Y.; Zong, Y.; Han, M.; Huang, D. J. *Small* **2007**, *3*, 290–293.

JA904824W